



13th International Conference on Greenhouse Gas Control Technologies, GHGT-13, 14-18
November 2016, Lausanne, Switzerland

Pore space quantification of sedimentary rocks before-after supercritical CO₂ interaction by optical image analysis

Edgar Berrezueta^{a*}, María José Domínguez-Cuesta^b, Berta Ordóñez-Casado^a, Cristian
Medina^c, Ricardo Molinero^a

^aInstituto Geológico y Minero de España (IGME), C/Matemático Pedrayes 25, Oviedo 33005, Spain.

^bUniversidad de Oviedo, Departamento de Geología, C/Jesús Arias de Velasco s/n, Oviedo 33005, Spain.

^cIndiana Geological Survey, 611 North Walnut Grove Avenue, Bloomington, IN 47405, United States.

Abstract

Optical image analysis (OIA) allows a quantitative characterization of pore space measured through thin sections. Together with petrographic studies, by using optical microscopy (OpM), OIA could provide a reproducible pore characterization of sedimentary rocks in applications related to the geological storage of CO₂. This research is focused on the application of the OIA technique to measure porosity on thin section samples of sandstones from Spain before and after CO₂ injection to supercritical (SC) conditions in autoclave ($P \approx 7.5$ MPa and $T \approx 35$ °C). The aim of this article is to show preliminary measures by OIA using images acquired with high-resolution scanner (HRS). Mineral images were acquired from thin sections before and after SC-CO₂ injection. The optical measures of porosity on the thin sections of sandstones showed an effective pore segmentation considering different images in cross-polarized light conditions (90°/0°; 120°/30°) and plane-polarized light conditions (90°/-) of the same petrographic scene. Mineralogical studies by OpM and OIA-HRS have allowed an exhaustive characterization of the samples studied and a preliminary approximation of the CO₂-rock interactions. This study shows a fast, effective and reproducible methodology that allowed the researchers to obtain qualitative information about changes in the pore network (optical porosity) distribution on the thin section that could be applied to similar experimental injection tests.

© 2017 The Authors. Published by Elsevier Ltd. This is an open access article under the CC BY-NC-ND license (<http://creativecommons.org/licenses/by-nc-nd/4.0/>).

Peer-review under responsibility of the organizing committee of GHGT-13.

Keywords: reservoir characterization, reflection seismic, boreholes, 3D geological modelling, CO₂ storage ;

* Corresponding author. Tel.: +34 985-258-611; fax: +36 985-276-767.
E-mail address: e.berrezueta@igme.es

1. Introduction and Objectives

Carbon capture, utilization and sequestration (CCUS) is a way to reduce the atmospheric emission of greenhouse gases. Deep geological storage in porous rock formations is considered the most appropriate strategy for CO₂ sequestration [1-4] and injectivity is a key technical and economic issue for CCUS projects [5,6]. The feasibility of cost-effective geological sequestration is fundamentally dependent on local and suitable geological sequestration systems, including effective reservoir zones for injection and storage of CO₂ that acts as a seal for its confinement. To geologically store CO₂, it must first be compressed until reaching a denser fluid state known as supercritical (SC) [7]. The SC CO₂ injection in the subsurface depends mainly on the porosity and permeability of the host rock [6,8]. According to [9,10], CO₂ interactions with the host rock, such as dissolution or precipitation of minerals are important, as well as mineral trapping [11,12]. The dissolution of SC CO₂ into brine will control the rate of dissolution and precipitation of minerals constituting the porous rock. Volume changes during the solid phase will modify the pore structure, affecting both porosity and permeability of the porous media [13-15]. Measured changes, such as dissolution and/or precipitation induced by CO₂ injection into sedimentary rocks, show important information that could be used in real injection tests to model and estimate storage capacity [3-5,12,15]. Furthermore, mineralogical-scale changes (texture, mineralogy, and optical porosity) are also important preliminary data in CCUS projects [14,15].

Petrographic analysis of the thin sections by transmitted light microscopy is one of the main methods for rock characterization and classification. Optical image analysis (OIA) supporting microscopic observation can be applied to improve pore characterization of sedimentary rocks, providing accurate and representative numerical support to petrographic studies, under thin section scale [16-18]. Furthermore, this technique represents an important advancement over traditional techniques (point counting) used to automate the characterization of objects (minerals, pores, etc) in digital-images [17-21].

In order to quantify the present/visible pore system (i.e. pore space and pore shape) in thin sections by OIA, these samples were studied by totally scanning the mineralized area with a high-resolution scanner (HRS). The aim of this research is to establish an automated-image optical quantification protocol that allows pore system characterization of rocks exposed to SC CO₂, improving process developed by [22]. The objectives of this research are: i) definition of effective and reproducible methodology that allows researchers to obtain qualitative information about the pore network area and pore distribution to thin section scale; and ii) quantitative pore description (area, diameter, roundness, aspect and pore-size distribution) of the samples studied by OIA-HRS.

2. Materials and Methods

The procedures used for the identification and quantification of pores by OIA included three main steps [14,17,18] (Fig. 1): First, the representative samples and visual rock characterization yielding information about the basin studies were selected. Second, the pore characterization were set in place and comprised of textual and mineralogical studies (including pore characterization) of the sandstones by OpM and scanning electron microscope (SEM) in thin sections, which included a co-relation with preliminary studies and sample injections with SC CO₂ in a laboratory. Finally, the OIA quantification of the pores found in thin sections of sandstones were studied (using red, green and blue -RGB- image analysis on images acquired with HRS).

The samples for this study were collected from different sedimentary basins within Spain that offered favorable conditions for the study of CO₂ storage [23]. Three geological formations consisting of sandstones and potentially suitable for CO₂ sequestration were selected for this study (Fig. 2a). The three sandstone samples (S1, S2 and S3) were preliminary studied by [14,17,18]. They are proximal facies (located close to its source area i.e. short transport distance) and consist of: i) feldespatic Cretaceous sandstones from the Iberian Ranges in NNE Spain (Tiermes Formation), ii) greywacke Triassic sandstones from the Guadalquivir Basin in SE Spain (Linares-Manuel Formation), and iii) quartz-arenite Triassic sandstones from Duero Basin in NW Spain (Utrillas Formation).

The samples studied corresponded to contiguous sandstone blocks where the area studied corresponded to the more external part of sample blocks (Fig. 2b) before and after SC CO₂ injection ($P \approx 7.5$ MPa and $T \approx 35$ °C). The selected P-T conditions and runtimes of our experiments aimed to reproduce the reservoir rock dry-wet

environment, adjacent to a theoretical injection borehole [14,17,18]. Theoretical reservoir rock environment [13,24] and autoclave to reproduce rock environment [14,15,25] are shown in Fig. 2 c–d.

A HRS (CanonScan FS 4000 US) was used to acquire digital images. FilmGet FS is an Adobe Photoshop plugin that runs the scanner, providing a variety of image adjustments in image acquisition. HRS is an advanced photo system film scanner (cold cathode mercury fluorescent lamp, constant color intensity control and focus auto/manual -selectable-). Polarized filters (linear polarizers ST-38-40 Screen Tech) have been added so that images were scanned under crossed-polarizers. QGIS 2.12 Lyon is a cross-platform free and open-source and desktop geographic information system (GIS) used for geo-referencing raster image. ImageJ64 is an open-source image-processing program designed for scientific multidimensional images that include the latest tools used for the scientific image processing (capture, process, measure, share, visualize and compare). In this study, these steps have been included in the procedures defined for the identification and quantification of pores by OIA (Fig. 1).

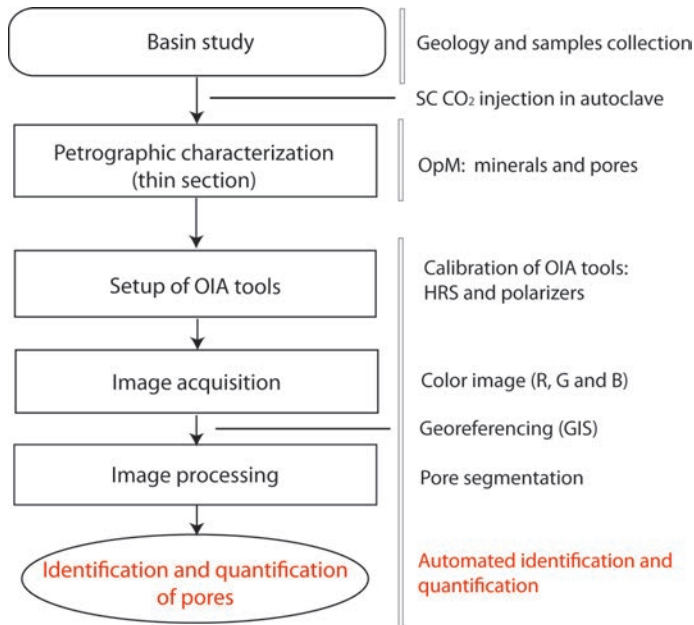


Fig. 1. Schematic representation of the sequence of optical pore identification and quantification using OIA-HRS. Modified from [14,17,18].

3. Preliminary studies

Three different types of sandstones were exposed to SC CO₂ conditions in autoclave. Three thin sections were characterized by applying OpM and SEM before and after SC CO₂ injection [14,17,18]. The mineralogy of samples (thin sections) S1 and S2, without SC CO₂ interaction is similar: quartz, K-feldspar, phyllosilicates (e.g. sericite and other clays), carbonate and less abundant biotite, muscovite, plagioclase, apatite, zircon and Fe-oxides. However, both samples show two different textures. Sample S1 is homogeneous and shows good sorting. Sample S2 is heterogeneous and has high porosity and permeability produced by an interconnected framework of micro-channels. The mineralogy of sample S3 without SC CO₂ interaction consists of quartz (> 95 %), very minor potassium feldspars (orthoclase) and a small amount of micas (muscovite and chlorite). Accessory minerals (1–5 %) are opaque minerals, such as iron oxides and hydroxides (hematite and limonite), disposed as aggregates. The grains range from moderately to poorly sorted in sample S3. According to the classification by [26,27], sample S1 is a Feldspathic sandstone; sample S2 is a Greywacke and sample S3 is a Quartz-arenite (> 95 % of quartz). Samples after SC CO₂ injection were also characterized applying OpM and SEM.

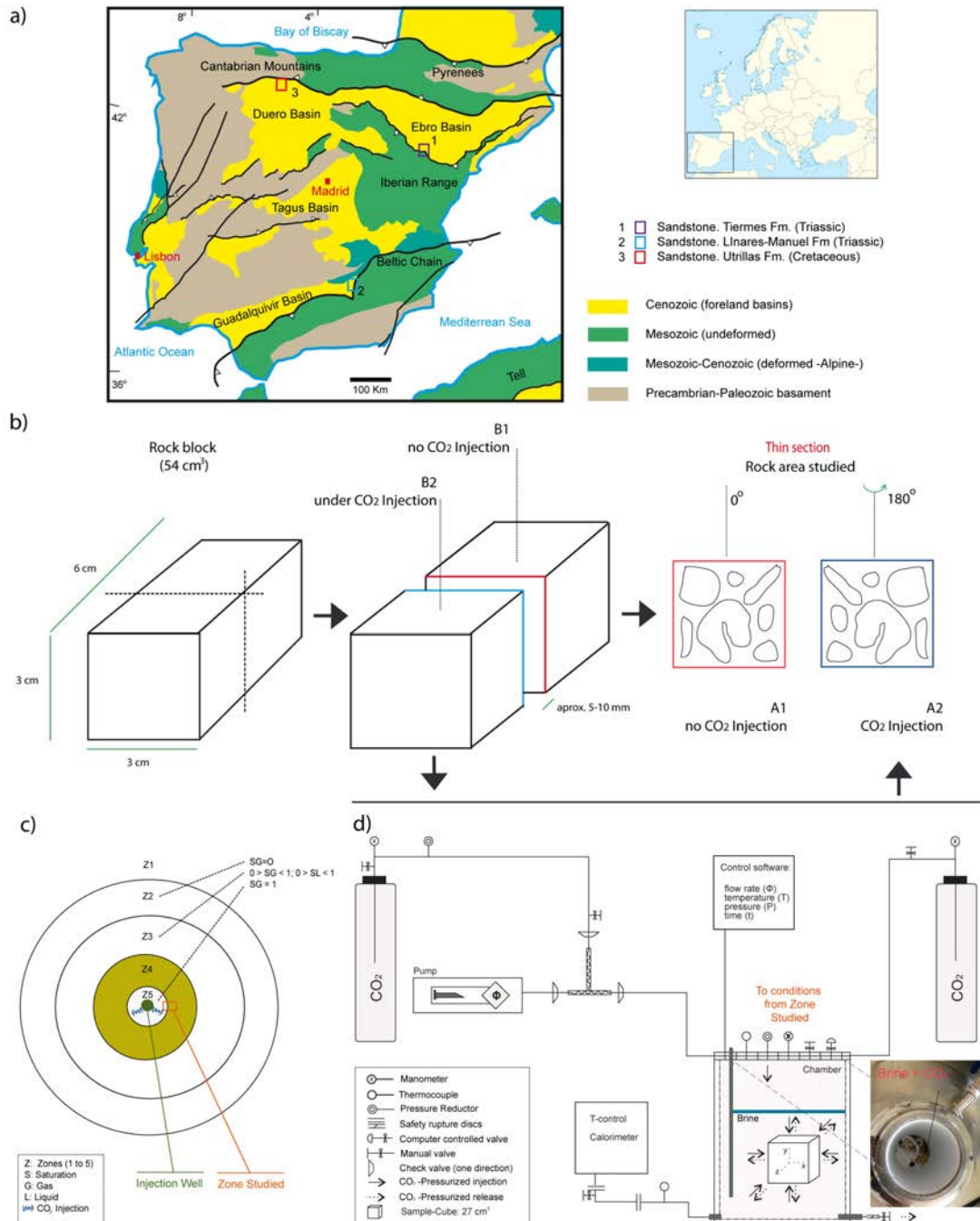


Fig. 2. (a) Location and regional geology of the areas selected for the borehole and sample collection. Modified from [18,28]; (b) schematic representation of two block samples studied and their thin sections [29]; (c) conceptual diagram of the reactive zones (Z1, Z2, Z3, Z4 and Z5) around the injection well according to [13,24]; (d) diagram of reactor system (autoclave) used for the pressurized CO₂ injection and reproduction of conceptual reactive zones in the injection well (e.g. CO₂ dry and CO₂-rich brine). Modified from [14-18].

In detail, one sample from Manuel Formation (S1CO₂) and other samples from Tiermes Formation (S2CO₂) were exposed to Dry SC CO₂ in autoclave (P ≈ 7.5 MPa, T ≈ 35 °C and t ≈ 1000 h exposure time). One Sample from Utrillas Formation (S3CO₂+B) was exposed to SC CO₂-rich brine (B) in autoclave (P ≈ 7.5 MPa, T ≈ 35 °C and t ≈ 24 h exposure time).

Previous studies with OpM and SEM techniques have allowed detecting qualitative changes in the pore network distribution (optical porosity) of the studied sandstones, based on the samples before SC CO₂ injection [17,18]. Furthermore, applying OIA on images acquired with the charge-coupled device (CCD) camera attached to OpM allowed researchers to measure the porosity changes [17-18] in the thin sections studied. In this preliminary quantification, sample S1 was studied by using the OIA-OpM at 10x the objective and considering a pore greater than 4 μm². Sample S2 was studied by using the OIA-OpM at 4x the objective and considering a pore greater than 24 μm². Sample S3 were studied by using the OIA-OpM at 10x the objective and considering a pore greater than 9 μm². Significant variation (porosity variation > OIA operator error: 1.24%) of porosity was established in the 3 cases (Table 1) which compared samples without CO₂ and samples exposed to SC CO₂. Basic information about the samples studied is summarized in Table 1.

Table 1. Basic information of samples studied from preliminary studies [17,22]. Total porosity of samples (three thin sections) measured by OIA-OpM.

| Rock Classification | Geological information | Before SC CO ₂ | | After SC CO ₂ | | Before-After | |
|-----------------------|---------------------------------------|---------------------------|------------|--------------------------|------------|--------------------|----------------|
| | | Sample | Porosity | Sample | Porosity | Porosity variation | Interpretation |
| Feldspathic Sandstone | Linares-Manuel Fm. Guadalquivir Basin | S1 | 12.63±0.16 | S1CO ₂ | 12.94±0.16 | 0.31 | No change |
| Greywacke | Tiermes Fm. Ebro Basin | S2 | 19.01±0.25 | S2CO ₂ | 21.16±0.26 | 2.15 | Increase |
| Quartz-arenite | Utrillas Fm. Duero Basin | S3 | 9.55±0.12 | S3CO ₂ +B | 11.13±0.14 | 1.75 | Increase |

4. Pore quantification by OIA-HRS

The pore network quantification by OIA-HRS was carried out in the same thin sections studied by OIA-OpM. In this case, the images were acquired with a resolution of ≈ 6.35 μm/pixel (Fig. 3). However, the researchers considered pores bigger than 4 pixels (ca. 160 μm² or 7.1 μm of radius). The quantification by OIA was applied on images acquired by HRS which allowed the researchers to quantify several interesting parameters related to size (e.g. area and diameter) and to pore shape (e.g. roundness and aspect ratio).

4.1. Image acquisition

For each of the thin sections 2 different pairs of filters (90°/0°; 120°/30°) with mutually orthogonal directions of polarization have been used. Furthermore, an additional image was acquired with only one filter of polarization (90°/-). The images were acquired (Fig. 3 and Fig. 4a) under a real optical resolution of 1574.80 pixels per cm (≈ 6.35 μm/pixel) supported for the scanner. This acquisition method allowed to scan the entire surface area of a thin section (≈ 2cm*3cm) and to archive it at once, in a single digitization process.

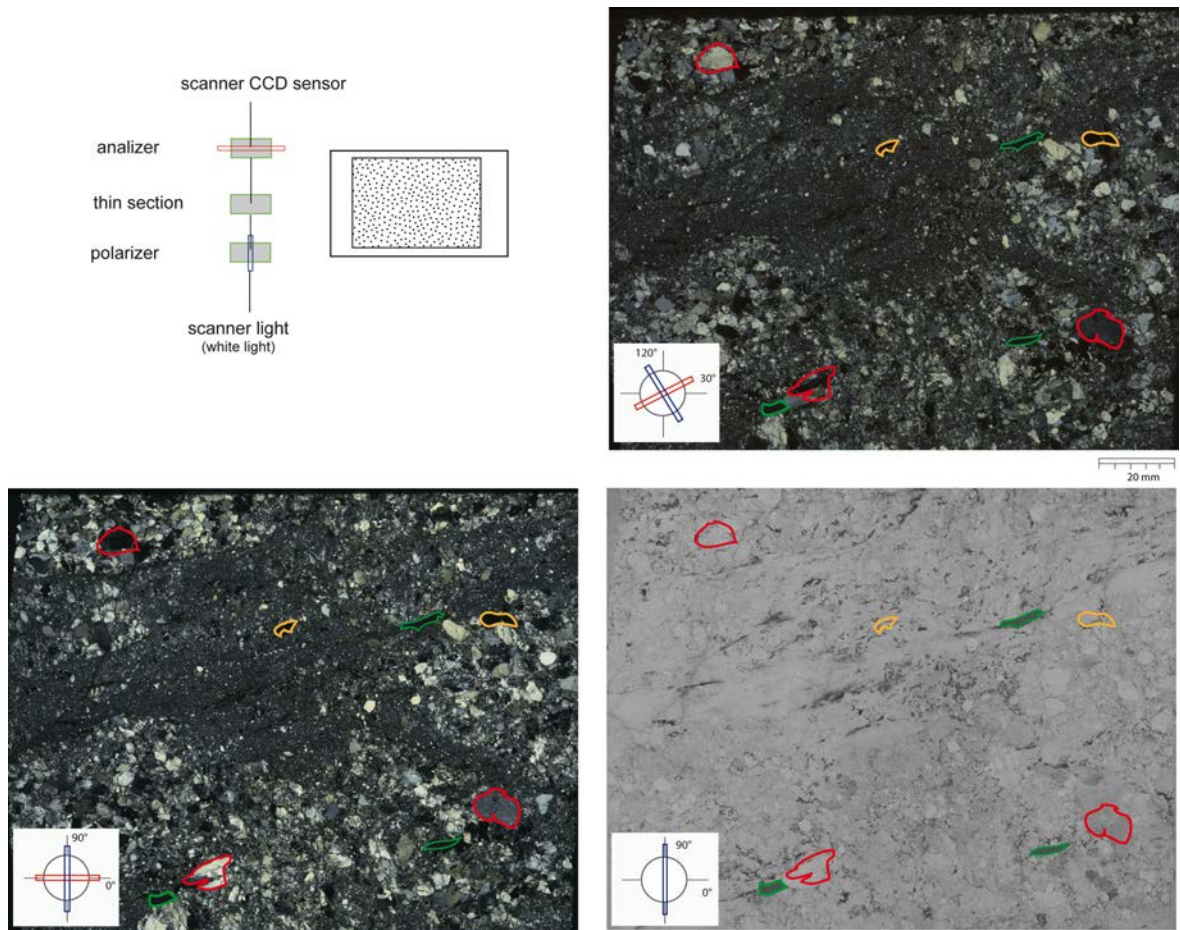


Fig. 3. Mineral images acquired by HRS under cross-polarized light and plane-polarized light conditions. Red polygons are anisotropic minerals, green polygons are opaque minerals and yellow ones are pores. Modified from [22].

4.2. Image pre-processing

Although the scanning process of the thin sections provides a set of images with XY coordinates, it is essential to ensure a very accurate spatial position of them. A process of assigning exact coordinates to each pixel of the raster image has been carried out (Fig.4b) by using QGIS (*Georeferencer GDAL plugin*) according to [22]. The first step is to assign coordinates to the first image, from a set of 3 images, assigning coordinates to 3 points -x and y pixels-. The remaining two images are georeferenced by using the first referenced image. To select common areas on the georeferenced image set, it has been applied a Clipping tool in QGIS. After this process, the set images will have the same information and the same size (Fig. 4c).

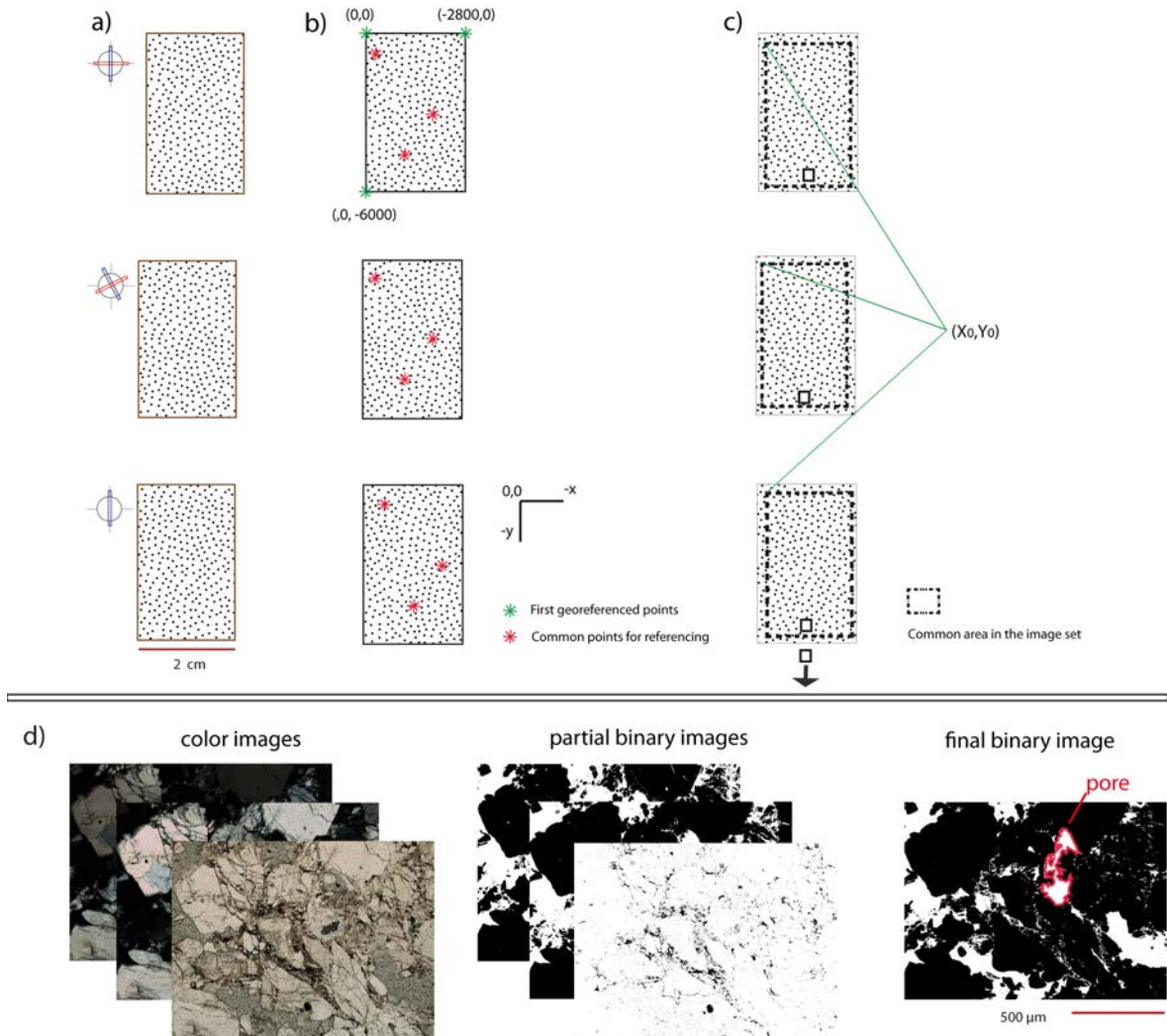


Fig. 4. Schematic work sequence: (a) Three images acquisition under polarized light by using HRS (2 under cross polarized light and one under parallel polarized light); (b) images geo-referencing; (c) selection of areas of interest on geo-referenced images set; (d) sequence of pore segmentation performed on color images (geo-referenced) where partial binary images were obtained by using pore segmentation ranges. Final binary image was obtained by the interception of partial binary images. Modified from [22].

4.3. Image segmentation

Gray level values of pores were calculated by using a supervised training step [17,22]. This was conducted by sampling Windows ($\approx 10 \times 10$ pixels) that were placed on a region that definitely was considered as a pore. Although pores displayed in HRS (emulating OpM) should be uncolored (black in crossed-polarizers and white in parallel ones) [17], a range of RGB values commonly appeared (Table 2). These ranges (Table 2) are normally used for the segmentation of pores in thin sections of sandstones (Fig. 4d) with the use of RGB images (3 combined GL images) and 3 distinct positions of image acquisition (2 under crossed polarizers and 1 under plane polarizer).

Table 2. Pore segmentation ranges (gray levels) for Red, Green and Blue bands of images acquired under cross-polarized and plane-polarized light conditions. Where χ is mean, σ is standard deviation and significance level for the ranges calculated is 99.9%. Based on [22].

| RGB Image | Pore in crossed polarized image | | | Pore in plane polarized image | | |
|-----------|---------------------------------|----------|-----------------------|-------------------------------|----------|-----------------------|
| | χ (Gray level) | σ | Range (Gray level) | χ (Gray level) | σ | Range (Gray level) |
| Red | 28.25 | 10.62 | [0 - 60] | 223.16 | 12.66 | [185 - 255] |
| Green | 26.43 | 9.66 | [0 - 55] | 229.53 | 13.17 | [190 - 255] |
| Blue | 31.71 | 10.93 | [0 - 65] | 236.43 | 6.99 | [215 - 255] |

4.4. Pore quantification by OIA-HRS

Once the porosity was defined, the most appropriate mineral features for assessing their size and shape were selected. The main size parameters considered were i) the area (A), ii) the major and minor axis (primary and secondary axis of the best fitting ellipse) and iii) perimeter (P). Pore particles were considered when their size was bigger than 4 pixels (ca. $160 \mu\text{m}^2$). The main shape parameters considered were roundness (Ro, equation 1) and aspect ratio (As, equation 2). Roundness is the measurement of how circular an object is and Aspect ratio is the ratio of the axes of the pores-fitted ellipse, where major and minor are the primary and secondary axis of the best fitting ellipse. A percentage of pore area measured by OIA-HRS for the samples S1 to S3 and S1CO₂ to S3CO₂+B are shown in Table 3.

$$Ro = \frac{4 \cdot \pi \cdot A}{P^2} \quad (1)$$

$$As = \frac{MajorAxis}{MinorAxis} \quad (2)$$

Table 3. Total porosity, Roundness (Ro) and Aspect ratio (As) of sandstone thin sections (before and after SC CO₂ injection) measured by OIA-HRS. Variation (Δ) in %.

| Thin section | Porosity % | Porosity Change | Ro | Δ Ro | As | Δ As |
|-------------------|---------------|--------------------|-------|-------------|-------|-------------|
| S1 | 13.62±0.17 | 0.78 | 0.607 | -0.73 | 2.157 | -2.31 |
| S1CO ₂ | 14.40±0.18 | | 0.602 | | 2.107 | |
| S2 | 18.61±0.23 | 1.99 | 0.610 | -2.75 | 2.167 | 3.64 |
| S2CO ₂ | 20.60±0.26 | | 0.593 | | 2.246 | |
| S3 | 15.44±0.20 | 1.29 | 0.570 | -3.99 | 2.110 | -2.80 |
| S3CO ₂ | 16.73±0.21 | | 0.540 | | 2.050 | |

In Table 3, it can be also noticed distinct pore variation caused for SC CO₂ injection in samples studied and pore parameters characterization and their variations (roundness and pore aspect ratio). The statistical analysis of pore values measured (e.g. pore diameter), comparing samples before and after SC CO₂ injection, shows a variation of the average and standard deviation: feldspatic sandstone sample (6 and -8% respectively) greywacke sample (16 and 28% respectively) and quartz-arenite sample (-10 and 8% respectively). In the case of pore features such as roundness and aspect ratio, when comparing samples before-after SC CO₂ injection, the parameters have changed (Table 3). For feldspathic sandstone sample, both roundness and aspect decreased with CO₂ interaction (0.73% and

2.30%, respectively). In the case of the greywacke sample, roundness decreased with CO₂ interaction (2.75%) but the aspect ratio increased (3.64%). Finally, for quartz-arenite sample (Fig. 5), both roundness and pore aspect ratio decreased with CO₂ interaction (3.99% and 2.80% respectively).

5. Discussion

OIA as a mineralogical quantification tool presents an important advancement in petrographic studies [19], specifically in quantifying different aspects of the porosity in thin sections [14,30]. As shown in previous researches, the automated quantification of mineral phases by digital techniques [17,31] is appropriate for systematic and automatic mineral quantification from thin sections.

The application of OIA-HRS has allowed to perform a complete characterization of all pores (optical pores) in the thin sections studied. The OIA-HRS process applied has ensured that the entire thin section studied was digitalized (Fig. 5). A general procedure to automatize the image analysis was developed, adapting the procedures described by [21,32] and algorithms described by [17], in order to quantify the textural and porosity changes (area, roundness of minerals/pores, pore size distribution) due to experimental CO₂ injection. In addition, a Georeferencing process (GIS software: QGIS) applied to the images scanned from thin sections [22] was applied to provide a set of images with a high spatial precision (x, y). GIS software ensured that the same information in the thin sections was present in all images used during the analysis.

The mineral images acquired using HRS and OIA software, considering images acquired under cross-polarized light (90°/0°; 120°/30°) and plane-polarized light (90°/-) conditions allowed to achieve an appropriate segmentation (identification) of the porous system of the whole petrographic scene studied [22]. Furthermore, OIA software allowed to measure each pore space and its attributes such as area, size, aspect ratio and other pore shape parameters.

The results obtained (optical pore changes) both, before and after the experimental injection of CO₂, could be interpreted as a textural and mineralogical evolution from the untreated samples to the treated ones [14,17,18]. Since the mineralogy in the feldspathic sandstones and greywacke samples are similar in the three cases studied, the original rock texture is more than likely what promoted the varied effects when CO₂ is injected. In the case of the quartz-arenite samples, where mineralogy and texture differ from the two sandstone samples, the original rock texture and mineralogy is more than likely what promoted the varied effects when CO₂ is injected. It is important to consider that pores smaller than 160 μm² have not been included in the measures of optical porosity, pore shapes parameters and pore size distribution, in the cases studied.

Furthermore, for more detailed studies, other important variables to evaluate the evolution of optical porosity after SC CO₂ injection in rock samples are: type of CO₂ injected (dry o wet) and injection process (flow, no flow, exposition time, etc.).

In a comparison of measures obtained by OIA-HRS (Table 3) with preliminary studies by OIA-OpM (Table 1), similar values (% pore area of samples and variation of pore area) were obtained compared to the samples shown before-after SC CO₂ interaction. It is worth noting that the time it took to process the OIA-HRS per sample (entire thin section) took about 2 hr while OIA-OpM (entire thin section) took about 30 hr per sample. Nevertheless, OIA-HRS process produced a resolution of ≈ 6.35 μm/pixel while OIA-OpM process had a resolution of ≈ 0.624 μm/pixel (e.g. magnification 10x).

Some improvements may make the method more efficient, such as: i) measuring the contribution of small pores to the total porosity (using HRS with higher resolution); ii) inclusion of automatic controller of polarizer's angle in the HRS; or iii) inclusion of a new polarization light condition (e.g. 150°/60°) during the acquisition process to improve the segmentation process.

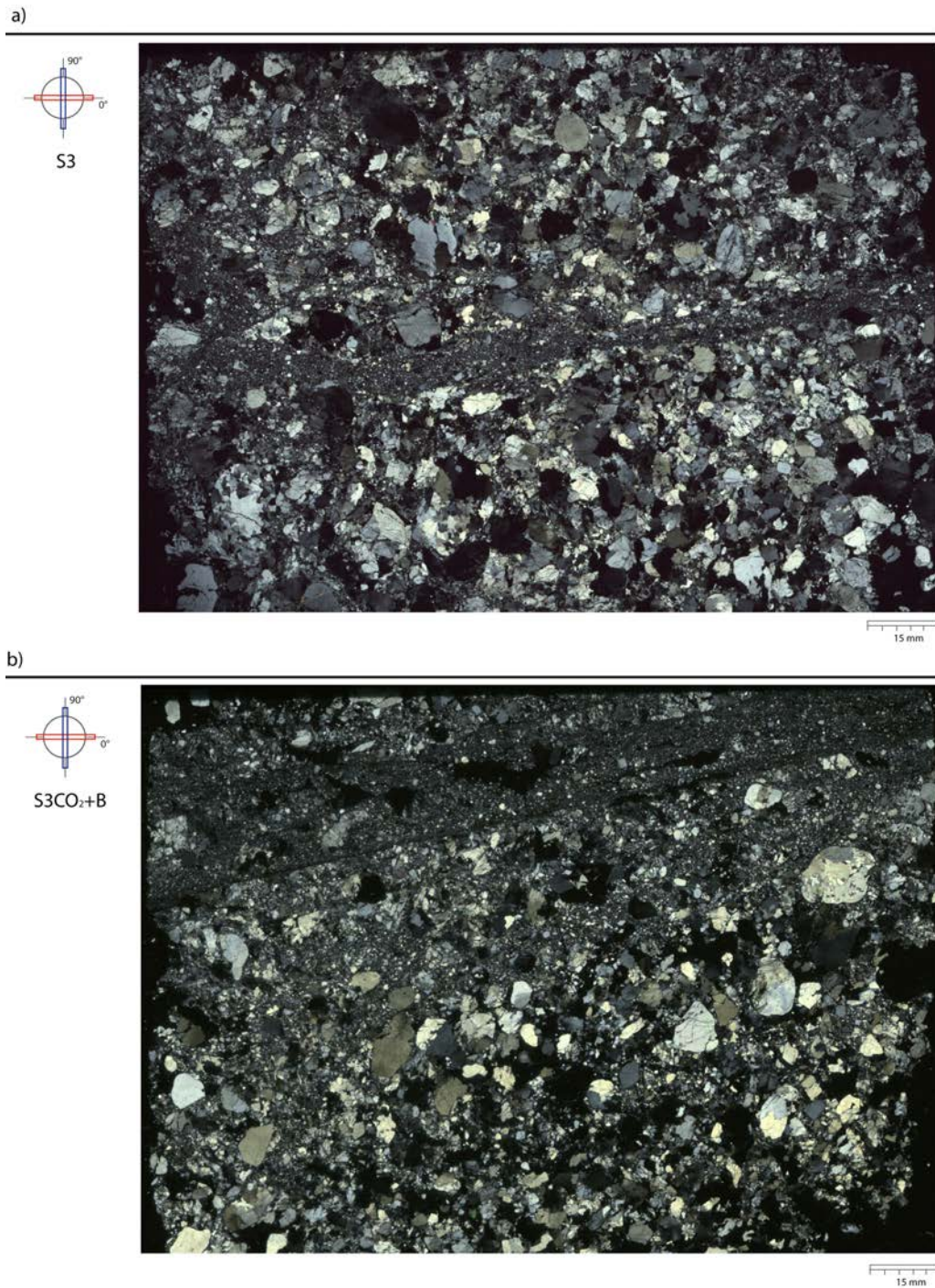


Fig. 5. Totally thin sections images taken under cross-polarized (90°/0°) light conditions with HRS (a) sample S3 (Quartz-arenite sample before SC CO₂ interaction) and (b) sample S3CO₂+B (Quartz-arenite sample before SC CO₂ interaction). Images acquired with 6.35 μm/pixel optical resolution.

6. Conclusions

The methodology developed in this work of OIA on image acquired with HRS constitutes a contribution to petrographic microscope analysis. The OIA-HRS process was successfully applied to three samples: a feldspathic sandstone, a greywacke and a quartz-arenite. All samples were selected due to their potential as CO₂ reservoirs in Spain. The precise pore segmentation in these samples (3 before SC CO₂ and 3 after SC CO₂ injection) proved to be highly effective for the identification and measurement of changes in the pore network (considering pores bigger than 160 μm²). Regarding the results obtained, OIA-HRS method provided the researchers with a quantitative data of the pore system and geometrical features from each pore space where fissures networks could be frequent and could not be easily quantified by standard OIA-OpM. Porosity increased for all three samples after interaction with SC CO₂ and no major mineralogy-textural changes were found. When comparing samples before and after SC CO₂ injection, we observed that optical porosity measured in the thin sections studied showed an average increase of total porosity of ≈ 1.5 %. The general process defined (protocols of image acquisition and pore segmentation) could be used on images acquisition with different devices and processing units than those applied in this study for pore network area and pore size distribution quantification.

Nomenclature

| | |
|----------|---|
| OIA | Optical Image Analysis |
| OpM | Optical Microscopy |
| SC | Supercritical |
| HRS | High Resolution Scanner |
| CCUS | Carbon Capture, Utilization and Storage |
| SEM | Scanning Electron Microscope |
| GIS | Geographic Information System |
| CCD | Charge-Coupled Device |
| RGB | Red, Green, Blue |
| B | Brine |
| χ | Mean |
| σ | Standard Deviation |
| GL | Grey Level |
| A | Area |
| P | Perimeter |
| Δ | Variation |
| Ro | Roundness |
| As | Aspect ratio |

Acknowledgements

The authors would like to thank the funding provided through the ALGECO2-IRMC Project (Instituto Geológico y Minero de España: 2294-2013), CO₂-Pore Project (Plan Nacional de España: 2009-10934, FEDER-UE). Thanks are due to José Luis García Lobón, Roberto Martínez Orio, Lope Calleja Escudero and Angel Rodríguez Rey for providing help in OIA techniques, images acquisition with HRS and statistical treatment of rock sample's analysis.

References

- [1] Bachu S. Sequestration of CO₂ in geological media: criteria and approach for site selection in response to climate change. *Energ. Convers. Manage* 2000; 41:953-970.
- [2] Benson SM, Cole DR. CO₂ sequestration in deep sedimentary formations. *Elements* 2008; 4:325-331.
- [3] Gaus I. Role and impact of CO₂-rock interactions during CO₂ storage in sedimentary rocks, *Int. J. Greenh. Gas Con* 2010; 4:73-89.

- [4] Izgec O, Demiral B, Bertin HJ, Akin S. CO₂ injection into saline carbonate aquifer formations I: laboratory investigation. *Transport in Porous Media* 2008; 72:1-24.
- [5] Bacci G, Korr A, Durucan S. Experimental investigation into salt precipitation during CO₂ injection in saline aquifers. *Energy Procedia* 2011; 4:4450-4456.
- [6] Medina CR, Rupp JA, Barnes DA. Effects of reduction in porosity and permeability with depth on storage capacity and injectivity in deep saline aquifers: A case study from the Mount Simon Sandstone aquifer. *Int. J. Greenh. Gas Con* 2011; 5:146-156.
- [7] Intergovernmental Panel on Climate Change (IPCC), In: Metz, B., Davidson, O., de Coninck, H.C, Loos, M., Meyer, L.A. (Eds.), *Special Report on Carbon Dioxide Capture and Storage* 2005; Cambridge University Press, Cambridge, UK/New York, USA, p. 442.
- [8] Zhang L, Soong Y, Dilmore R, Lopano C. Numerical simulation of porosity and permeability evolution of Mount Simon sandstone under geological carbon sequestration conditions. *Chem. Geol* 2015; 403:1-12.
- [9] Saedi A, Rezaee R, Evans B, Clennell B. Multiphase flow behaviour during CO₂ geo-sequestration: Emphasis on the effect of cyclic CO₂-brine flooding. *J. Petrol. Sci. Engin* 2011; 79:65-85.
- [10] Sayegh SG, Krause FF, Girard M, DeBree C. Rock/fluid interactions of carbonated brines in a sandstone reservoir: Pembina Cardium, Alberta, Canada, *SPE Formation Evaluation* 1990; 5:399-405.
- [11] Kaszuba JP, Janecky DR, Snow MG. Carbon dioxide reaction processes in a model brine aquifer at 200 °C and 200 bars: implications for geologic sequestration of carbon. *Appl. Geochem* 2003; 18:1065-1080.
- [12] Rosenbauer RJ, Koksalan T, Palandri JL. Experimental investigation of CO₂-brine-rock interactions at elevated temperature and pressure: implications for CO₂ sequestration in deep saline aquifers. *Fuel Proc. Technol* 2005; 5:146-156.
- [13] André L, Audigane P, Azaroual M, Menjoz A. Numerical modelling of fluid-rock chemical interactions at the supercritical CO₂-liquid interface during CO₂ injection into a carbonate reservoir, the Dogger aquifer (Paris Basin, France). *Energy Convers. Manage* 2007; 48:1782-1797
- [14] Berrezueta E, González-Menéndez L, Breitrner D, Luquot L. Pore system changes during experimental CO₂ injection into detritic rocks: Studies of potential storage rocks from some sedimentary basins of Spain. *Int. J. Greenh. Gas Con* 2013; 17:411-422.
- [15] Luquot L, Gouze P. Experimental determination of porosity and permeability changes induced by injection of CO₂ into carbonate Rocks. *Chem. Geol* 2009; 265:148-159.
- [16] Asmussen P, Conrad O, Günther A, Kirsch M, Riller U. Semi-automatic segmentation of petrographic thin section images using a “seeded-region growing algorithm” with an application to characterize weathered subarkose sandstone. *Comput. Geosci* 2015; 83:89-99.
- [17] Berrezueta E, González-Menéndez L, Ordoñez-Casado B, Olaya P. Pore network quantification of sandstones under experimental CO₂ injection using image analysis. *Comput. Geosci* 2015; 77:97-110.
- [18] Berrezueta E, Ordoñez-Casado B, Quintana L. Qualitative and quantitative changes in detrital reservoir rocks caused by CO₂-brine-rock interactions during first injection phases (Utrillas sandstones, northern Spain). *Solid Earth* 2016; 7(1):37-53.
- [19] Ehrlich R, Crabtree SJ, Kennedy SK, Cannon, RL. Petrographic image analysis I: analyses of reservoir pore complexes. *J. Sediment. Petrol* 1984; 54:1365-1378.
- [20] Fueten FA. Computer-controlled rotating polarizer stage for the petrographic microscope. *Comput. Geosci* 1997; 23(2):203-208.
- [21] Sardini P, Moreau E, Sammartino S, Touchard G. Primary mineral connectivity of polyphasic igneous rocks by high-quality digitisation and 2D image analysis. *Comput. Geosc* 1999; 25:599-608.
- [22] Berrezueta E, Domínguez-Cuesta MJ. Quantification of sandstone pore system by optical image analysis through high-resolution scanner images. IX Congreso Geológico de España 2016; Huelva, Spain, September 12-14, 2016.
- [23] García-Lobón JL, Reguera-García MI, Martín-León J, Rey-Moral C, Berrezueta E. Plan de selección y caracterización de áreas y estructuras favorables para el almacenamiento geológico de CO₂ en España. Resumen ejecutivo. Instituto Geológico y Minero de España (IGME), Madrid, 2010.
- [24] Gaus I. Role and impact of CO₂-rock interactions during CO₂ storage in sedimentary rocks. *Int. J. Greenh. Gas Con* 2010; 4, 73–89.
- [25] Tarkowski R, Wdowin M. Petrophysical and mineralogical research on the influence of CO₂ injection on Mesozoic reservoir and caprocks from the polish lowlands, *Oil Gas Sci. Technol. Revue d’IFP Energies Nouvell* 2011; 66:137-150.
- [26] Folk RL. *Petrology of Sedimentary Rocks*. Hemphill’s, Austin, Texas, 170 pp. 1974.
- [27] Pettijohn FJ, Potter PE, Siever R. *Sand and Sandstones*. Springer, Berlin, 553 pp. 1987.
- [28] Quintana L, Pulgar JA, Alonso JL. Displacement transfer from borders to interior of a plate: a crustal transect of Iberia. *Tectonophysics* 2015; 663:378-398.
- [29] Berrezueta E, González-Menéndez L, Ordoñez-Casado B, Luquot L, Quintana L, Gallastegui G, Martínez R, Olaya P, Breitrner D. Optical Image Analysis Applied to Pore Network Quantification of Sandstones Under Experimental CO₂ Injection. AGU Fall Meeting 2015; San Francisco, USA, December 14-18, 2015.
- [30] Clelland WD, Kantorowicz JD, Fens TW. Quantitative analysis of pore structure and its effects on reservoir behaviour: Upper Jurassic Ribble Member sandstones, Fulmar Field, UK North Sea. Form Ashton, M (ed.), *Advances in Reservoir Geology*, Geological Society Special Publications 1993; 69:57-79.
- [31] Anselmetti F, Luthi S, Eberli GP. Quantitative Characterization of Carbonate Pore Systems by Digital Image Analysis. *AAPG Bulletin* 1998; 82 (10):1815-1836.
- [32] Tarquini S, Favalli MA. Microscopic information system (MIS) for petrographic analysis. *Comput. Geosci* 2010; 36:665-674.